ESR Investigation of Tyrosyl Radicals of Prostaglandin H Synthase; Relation to Enzyme Catalysis

ARTICLE *in* JOURNAL OF BIOLOGICAL CHEMISTRY · NOVEMBER 1991

Impact Factor: 4.57 · DOI: 10.1007/978-1-4615-3520-1_12 · Source: PubMed

THE JOURNAL OF BIOLOGICAL CHEMISTRY

Vol. 266, No. 30, Issue of October 25, pp. 20045-20055, 1991
Printed in U.S.A.

Electron Spin Resonance Investigation of Tyrosyl Radicals of Prostaglandin H Synthase

RELATION TO ENZYME CATALYSIS*

(Received for publication, April 26, 1991)

Gunter Lassmann‡§, Rebecca Odenwaller¶, John F. Curtis‡, Janice A. DeGray‡, Ronald P. Mason‡, Lawrence J. Marnett¶, and Thomas E. Eling‡‖

From the ‡Laboratory of Molecular Biophysics, National Institute of Environmental Health Sciences, National Institutes of Health, Research Triangle Park, North Carolina 27709 and the ¶A. B. Hancock, Jr. Memorial Laboratory for Cancer Research, Center in Molecular Toxicology, Departments of Biochemistry and Chemistry, School of Medicine, Vanderbilt University, Nashville, Tennessee 37232-0146

We have examined, by low temperature ESR, the protein-derived radicals formed by reaction of purified ram seminal vesicle prostaglandin H synthase (PHS). Upon addition of arachidonic acid or 5-phenyl-4-pentenyl-1-hydroperoxide (PPHP) to PHS reconstituted with Fe(III)-protoporphyrin IX (Fe-PHS) at −12 °C, an ESR spectrum was observed at −196 °C containing a doublet that rapidly converted into a singlet. These protein-derived radicals were identified as tyrosyl radicals. The addition of a peroxidase substrate, phenol, completely abolished the appearance of the doublet and suppressed the formation of the singlet but did not inhibit eicosanoid formation. Incubation of arachidonic acid with PHS reconstituted with Mn(III)-protoporphyrin IX (Mn-PHS) produced only a broad singlet that exhibited different power saturation behavior than the tyrosyl radicals and decayed more rapidly. This broad singlet does not appear to be a tyrosyl radical. No ESR signals were observed on incubation of PPHP with Mn-PHS, which has cyclooxygenase but not peroxidase activity. Eicosanoid synthesis occurred very rapidly after addition of arachidonic acid and was complete within 1 min. In contrast, the protein-derived radicals appeared at a slower rate and after the addition of the substrate reached maximal levels between 1 and 2 min for Fe-PHS and 4–6 min for Mn-PHS. These results suggest that the observed protein-derived radicals are not catalytically competent intermediates in cyclooxygenase catalysis by either Fe-PHS or Mn-PHS. The peroxidase activity appears to play a major role in the formation of the tyrosyl radicals with Fe-PHS.

Prostaglandin H synthase (PHS)[1] catalyzes the oxygenation of arachidonic acid to prostaglandin endoperoxides, the initial step in prostaglandin, thromboxane, and prostacyclin biosynthesis (2–4). The amino acid sequences of mouse, sheep, and human PHSs are highly conserved (1, 5–7). The protein purified from sheep seminal vesicle microsomes is a glycoprotein composed of two 70-kDa subunits (8). It contains iron(III)-protoporphyrin IX as the prosthetic group at an apparent stoichiometry of 1/subunit (9–11). PHS exhibits two catalytic activities: a cyclooxygenase that oxygenates arachidonic acid to a hydroperoxide, and a peroxidase that reduces the hydroperoxide to an alcohol in the presence of a reducing substrate (12).

The mechanism by which PHS oxidizes arachidonic acid is of considerable interest. Removal of the 13-*pro*-*S*-hydrogen atom proceeds with a sizable isotope effect, indicating it is the rate-limiting step (13). The immediate product of hydrogen removal, a carbon-centered radical, has been trapped with 2-methyl-2-nitrosopropane (14, 15). Conversion of this carbon-centered radical to PGG_2 occurs by sequential coupling to O_2, serial cyclization, coupling to O_2, and reduction (16). The role of the enzyme in the overall transformation may be restricted to the initial stereoselective hydrogen removal (Equation 1) (17). The identity of the oxidizing agent responsible for this step is uncertain. Attention initially focused on the metal center as a likely candidate, in particular, on higher oxidation states of the heme prosthetic group produced during the peroxidase catalytic cycle (18, 19). The peroxidase of PHS is similar in function to other heme peroxidases in that it exists in the ferric state in the resting enzyme and is oxidized to the ferryl state by hydroperoxide substrates (Scheme 1) (18). One mechanistic possibility is that one or both of the ferryl-oxo complexes are oxidants in the cyclooxygenase reaction. Such a mechanism implies a synergism between the cyclooxygenase and peroxidase reactions and is consistent with the ability of agents that reduce hydroperoxides to inhibit cyclooxygenase activity as well as the ability of trace amounts of PGG_2 and fatty acid hydroperoxides to activate cyanide-inhibited cyclooxygenase (20, 21).

Another mechanistic possibility is that a peroxidase ferryl-oxo complex oxidizes an amino acid residue on the protein to

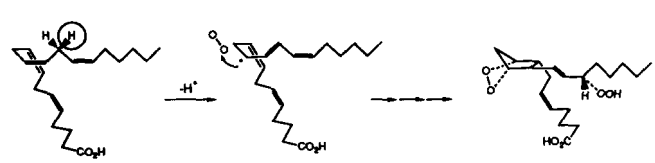

Equation 1

* This work was supported in part by National Institutes of Health Grant CA-47479. A portion of this work was presented at the 1991 meeting of the Federation of American Societies for Experimental Biology, Atlanta, GA. The costs of publication of this article were defrayed in part by the payment of page charges. This article must therefore be hereby marked "*advertisement*" in accordance with 18 U.S.C. Section 1734 solely to indicate this fact.

§ Present address: Central Institute of Molecular Biology, O-1115 Berlin-Buch, Germany.

‖ To whom correspondence should be addressed.

[1] The abbreviations used are: PHS, prostaglandin H synthase; Fe-PHS, PHS reconstituted with Fe(III)-protoporphyrin IX; Mn-PHS, PHS reconstituted with Mn(III)-protoporphyrin IX; PPHP, 5-phenyl-4-pentenyl-1-hydroperoxide; GC/MS, gas chromatography/mass spectrometry; PG, prostaglandin; W, watt(s); HPLC, high pressure liquid chromatography; HETE, hydroxyeicosatetraenoic acid.

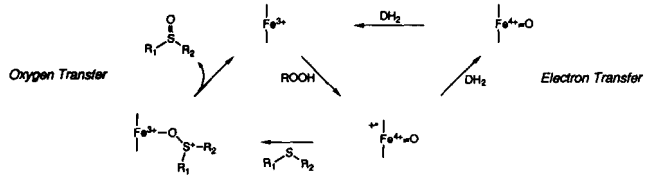

SCHEME 1. **Peroxidase catalytic cycle.**

a derivative that is the oxidizing agent for arachidonic acid. Ruf and colleagues (22, 23) detected a protein-derived radical by ESR spectroscopy after the addition of arachidonic acid or hydroperoxides to PHS. They identified this species as a tyrosyl radical by comparison of its spectral properties with the stable tyrosyl radical of ribonucleotide reductase (22, 24, 25). The hypothesis that this tyrosyl radical is the oxidizing agent for the cyclooxygenase reaction is attractive because it explains how a single heme group could participate in two different catalytic reactions on each protein subunit (Scheme 1). It also provides a mechanism by which a single peroxidase turnover could lead to multiple cyclooxygenase turnovers. The latter is important because derivatives of PHS exist (*e.g.* Mn-PHS) in which the cyclooxygenase activity is intact but the peroxidase activity is very low or undetectable (26–29).

Tyrosyl radicals of PHS are produced transiently after the addition of arachidonic acid or PGG_2 to resting enzyme. A doublet signal appears immediately after mixing but decays rapidly (~1 min) on standing at −12 °C (22, 30). Concomitant with decay of the doublet, a singlet ESR signal appears that persists and is detectable even at room temperature (31, 32). The singlet signal also appears to be caused by a tyrosyl radical but one in which the dihedral angle between the phenyl ring and the benzylic carbon is altered relative to the doublet (30).

Although it is clear that one or more tyrosyl radicals are produced as a result of the action of PHS, their role as catalytically competent intermediates in the cyclooxygenase reaction remains to be established. In particular, it is important to determine whether their formation is essential for cyclooxygenase catalysis or reflects a side reaction that occurs concomitant with catalysis. Tetranitromethane nitrates 1–3 tyrosine residues on PHS, rapidly inactivates cyclooxygenase activity, and prevents ethyl hydroperoxide-dependent formation of the doublet ESR signal (30, 33). Site-directed mutagenesis of Tyr^{385} to phenylalanine abolishes cyclooxygenase but not peroxidase activity, implying a critical role for this tyrosine residue in cyclooxygenase catalysis (33).[2] However, it is not known if the radical signals described above are derived from Tyr^{385}.

In the experiments described in the present report we investigated the production of protein-derived radicals as detected by low temperature ESR of PHS in which the heme prosthetic group was replaced with manganese protoporphyrin IX (Mn-PHS). Mn-PHS exhibits cyclooxygenase but little or no peroxidase activity, which provides a tool for detecting radicals associated only with cyclooxygenase activity. As a complement to these experiments, we used Fe-PHS and attempted to minimize the contribution of peroxidase activity to radical generation by carrying out arachidonic acid oxygenation in the presence of a peroxidase reducing substrate, phenol. Finally, we compared the time course[3] of radical production with the time course of metabolism of radiolabeled arachidonic acid by Fe-PHS and Mn-PHS at −12 °C. The results of these experiments question the importance of spectroscopically detectable tyrosyl radicals to the cyclooxygenase catalytic cycle.

[2] Numbering of individual residues refers to the translation start site of ovine PHS (1).

EXPERIMENTAL PROCEDURES

Materials—Arachidonic acid was obtained from Nu Chek Prep (Elysian, MN). Tween 20 (Surfact-Amps 20) was obtained from Pierce Chemical Co. Manganese protoporphyrin IX chloride was purchased from Porphyrin Products (Logan, UT). Hematin, diethyldithiocarbamate (sodium salt), Sephadex G-200-120, Sephadex G-25-150, deoxycholate (sodium salt), EDTA (free acid), glutathione (reduced form, free acid), and bovine serum albumin (98–99%, essentially fatty acid free) were all obtained from Sigma. 5-Phenyl-4-pentenyl-1-hydroperoxide (PPHP) was synthesized as described previously (34). Centricon 30 microconcentrators were purchased from Amicon (Danvers, MA).

PHS was isolated from ram seminal vesicle microsomes as described previously and stored at −80 °C in 50 mM Tris·HCl (pH 8) at 4 °C containing 300 μM diethyldithiocarbamate and 0.1% Tween 20 (35). Diethyldithiocarbamate is normally used for stabilizing the enzyme during storage but was removed for ESR studies because its ability to coordinate trace amounts of copper resulted in the formation of ESR signals that interfered with the detection of tyrosyl radicals (36, 37). Apo-PHS was prepared via a recently described gel filtration procedure with minor variations in the buffers (38). For each apo preparation, 10–15 mg of protein was loaded on a Sephadex G-200 column (180–200 ml). The equilibration and elution buffer was 100 mM Tris·HCl (pH 8 at 4 °C), 0.1% deoxycholate, 5 mM EDTA, and 5 mM glutathione. Removal of the cholate, glutathione, and EDTA was accomplished by chromatography on a Sephadex G-25 column (10–20-ml volume) equilibrated and eluted with 80 mM Tris·HCl (pH 8) at 4 °C and 0.1% Tween 20. Protein concentration was determined with the Bio-Rad assay using bovine serum albumin (in the same buffer as PHS) to construct the standard curve. The protein was 99–100% apo based on cyclooxygenase activities measured with and without the addition of heme. The specific activity of the apoenzyme ranged from 27 to 87 kilounits. (One unit is the amount of PHS necessary to consume 1 nmol of O_2/min.) The purity of apo-PHS was >99% as judged by sodium dodecyl sulfate-polyacrylamide gel electrophoresis, Coomassie Blue staining, and densitometric scanning.

Sample Preparation and Low Temperature Kinetics—Centricon 30 microconcentrators were used to concentrate 0.47–0.93 mg of apo-PHS to approximately 100 μl (67–133 μM PHS) for each ESR sample. Apoprotein was subsequently reconstituted with either hematin or manganese protoporphyrin IX chloride using a 1:1 molar ratio of porphyrin to 70-kDa subunit. Porphyrins were added to each 100-μl aliquot of 67–133 μM apoenzyme from a 1 mM porphyrin stock (in dimethyl sulfoxide). The porphyrins were then allowed to incubate with the apoenzyme for 10 min at 0 °C before any further sample manipulation. In cases requiring preincubation with phenol or indomethacin, incubation of the porphyrin with apoprotein was carried out for 5 min followed by the addition of phenol or indomethacin and another 5-min incubation. Indomethacin was added to the enzyme in 5 μl of a 2 mM stock solution (in ethanol). Phenol was added to the enzyme from either a 2 or 50 mM aqueous stock solution. Heat inactivation of PHS was achieved by incubating the enzyme at 70–80 °C for 7–10 min.

Tris·HCl (100 mM, pH 8.1) containing 75% (v/v) glycerol was bubbled with O_2 for 2 min. One hundred μl of this buffer was added to 100 μl of 67–133 μM reconstituted PHS in an Eppendorf tube. A 1–2-μl aliquot of each ESR sample was removed for cyclooxygenase assay prior to the addition of the glycerol buffer. The samples were then cooled to −12 °C in a thermostatted ethanol/water bath before

[3] The time courses of radical formation are approximate because the time was not recorded until the sample was completely thawed. This would tend to *underestimate* the time course of radical production and decay. Thus, the actual time course of radical appearance is probably slower than reported in the figures. This further enhances the discrepancy between the kinetics of radical appearance and arachidonic acid oxygenation. Similar spectra were recorded when a single sample was incubated for a given time and frozen as when a sample was frozen and thawed repeatedly until that time was reached.

transfer to cylindrical ESR tubes precooled in the −12 °C bath. A syringe with a long hypodermic needle was used to transfer the protein solution to the ESR tube. Using a Hamilton syringe with a second long needle, 10 μl of 100 mM arachidonic acid (in ethanol) was added to the 200-μl sample in the ESR tube at −12 °C. Mixing was accomplished by stirring with this needle. The final conditions for reaction at −12 °C were 34–75 μM reconstituted PHS, 5 mM arachidonate, 37% glycerol, 5–10% dimethyl sulfoxide, and 5–8% ethanol. The reaction was stopped at various time points by immersing the ESR tube in liquid nitrogen after removal of the ethanol from the sample tube by wiping with a Kimwipe. The shortest reproducible reaction time achieved at −12 °C was 10 s. After an ESR spectrum of the first time point, recorded at −196 °C, the sample tube was placed at −12 °C until the sample thawed, at which point the reaction time continued until the next time point. The sample was refrozen at −196 °C and the spectrum recorded. To accumulate data for kinetic curves of reaction times between 10 s and 22 min, this procedure was repeated with the same sample tube.

Reactions of PHS with PPHP were performed in a manner similar to that with arachidonate except 10 μl of 6.5 mM PPHP solution (in ethanol) was added to the assay instead of arachidonate. Final reaction conditions were 34–75 μM reconstituted PHS, 325 μM PPHP, 37% glycerol, 5–10% dimethyl sulfoxide, and 5–8% ethanol.

Assay of Cyclooxygenase Activity—O_2 consumption was monitored at 37 °C with a Gilson model 5/6 oxygraph equipped with a Clark electrode and a thermostatted cuvette. During enzyme preparation aliquots of PHS were assayed in a final volume of 1.3 ml containing 100 mM Tris·HCl (pH 8), 500 μM phenol, and 1 mM hematin. Arachidonic acid (100 μM final concentration) was added to initiate the cyclooxygenase reaction. During the preparation of samples for ESR, different cyclooxygenase assay conditions were used to check for cyclooxygenase activity just before addition of glycerol to each 5–9 mg/ml PHS solution. In these assays, the final volume of the reaction was 1.5 ml. Reaction was initiated by the addition of 100 μM arachidonate to the cuvette containing 100 mM potassium phosphate (pH 7.8), 500 μM phenol, and a 1–2 μl (5–19 μg) of PHS aliquot removed just before the sample was prepared for ESR.

ESR Technique and Spectra Evaluation—ESR spectra were recorded with a Bruker ESP 300 spectrometer using 2-mW microwave power and 3–8-gauss modulation amplitude. Sample volumes of 200 μl were contained in cylindrical quartz tubes (3-mm inner diameter) closed with caps and then placed in a finger cryostat (−196 °C) in a TM_{110} cavity. Protein-derived radical(s) for the Mn-PHS were also measured at higher temperatures using a gas flow cryostat accessory to control the temperature in the ESR cavity. ESR spectra for the Fe-PHS with arachidonic acid were also recorded at room temperature in a 17-mm flat cell for aqueous solutions. The installed data processing system, ESP 1600, was used for acquisition, accumulation, smoothing, base-line correction, double integration, and subtraction of spectra.

A freshly prepared aqueous glycerol solution of a stable nitroxide radical (TEMPOL) was frozen in the same cylindrical quartz tubes as the enzyme samples. Spectra were recorded at −196 °C and used as the absolute standard for spin concentration with computer double integration. The error (10–30%) in computer integration was caused mainly by uncertainties in the base line. The relative radical concentrations in the kinetic experiments were determined by comparison of amplitudes only (line shape unchanged), and the error was approximately 5%. At short reaction times the error associated with stopping the reaction by rapid freezing was slightly larger (10%). Spectral subtraction to estimate the percentage of pure singlet or doublet was performed by computer titration (subtraction of the pure singlet line shape from the experimental spectrum until the pure doublet remained).

ESR spectral simulation with anisotropic g- and hyperfine coupling tensors (powder spectra) were performed using a powder pattern simulation program (POW) part of the Brown University Powder Pattern Package (39, 40).

Low Temperature Metabolism of Arachidonic Acid—Apoprotein was reconstituted with either hematin or manganese protoporphyrin IX chloride as described above. Incubation mixtures were also prepared as described for low temperature ESR studies. The samples (final volume, 200 μl) were preincubated for 10 min at −12 °C. Reactions were initiated by the addition of 10 μl of 100 mM [^{3}H] arachidonic acid (20 mCi/mmol), containing 1.0 μCi of [^{3}H]PGB_2 (60 mCi/mmol) as an internal standard. Mixing was accomplished by briefly removing the sample from the −12 °C bath and vortexing. Twenty-μl aliquots of the incubation mixture were taken at predetermined time points and added to microcentrifuge tubes containing 150 μl of ethanol. The aliquots were allowed to stand at room temperature for 1 h to allow for decomposition of PGG_2 and PGH_2 to 15-hydroperoxy-PGE_2 and PGE_2, respectively. The aliquots were prepared for HPLC analysis by adding 127 μl of water and 3 μl of glacial acetic acid. The samples were then centrifuged (16,000 × *g*) for 5 min. Two hundred-μl aliquots were analyzed by reversed phase HPLC with a Beckman Ultrasphere column (4.6 mm × 25 cm) using a method described previously (41). Analysis was performed on a HPLC system consisting of the following Waters equipment: two model 6000A pumps, a model 710B WISP autosampler, and a model 721 system controller. Radioactivity was monitored with a Radiomatic model CR flow detector equipped with a 2.5-ml liquid flow cell. Ecolume (ICN Biochemicals, Irvine, CA) was used as the scintillant. Mass calculations were based on recovery of the internal standard.

Identification of 11-Hydroxyeicosatetraenoic Acid, 15-Hydroxyeicosatetraenoic Acid, and 12-Hydroxyheptadecatrienoic Acid—To identify positively the arachidonic acid metabolites that eluted at 60 and 70 min on reversed phase HPLC, preparative scale incubations were performed at −12 °C. For reasons of economy, ram seminal vesicle microsomes were used as the source of PHS (final concentration, 1.5 mg/ml). The total volume of the incubation was 20 ml. After a 10-min preincubation the reaction was initiated by the addition of 100 μl of 20 mM arachidonic acid. The reaction was terminated after 10 min by acidification with glacial acetic acid followed immediately by solid phase extraction utilizing a pair of Prep-Sep C-18 columns (Fisher Scientific). The columns were washed with 10 ml of 0.1% acetic acid to remove glycerol. The eicosanoids were then eluted by washing each column with 5 ml of methanol. The methanol fractions were pooled and the solvent removed by rotary evaporation. The sample was reconstituted in 1.0 ml of 50:50:1 methanol:water:acetic acid and analyzed by reversed phase HPLC. On-line UV spectra were obtained using a Waters model 990 photodiode detector. Two fractions were collected and saved for GC/MS analysis.

Samples were evaporated to dryness and derivatized for GC/MS analysis. The samples were initially treated with 200 μl of ethereal diazomethane. The reagent was removed, and the samples were redissolved in methanol and catalytically hydrogenated as described previously. After removal of solvent and catalyst, the samples were treated with 40 μl of bis(trimethylsilyl)trifluoroacetamide for 30 min at 60 °C. GC/MS analysis was performed using a Kratos Concept 1s mass spectrometer equipped with a 15-m DB-1 column (0.25-mm inner diameter, 0.1-μm film thickness). Helium was used as the carrier gas at a linear velocity of 25 cm/s. After 1 min at an initial temperature of 180 °C, the oven temperature was increased at 10 °C/min to a final temperature of 325 °C and held for 5 min. Mass spectra were obtained in the EI mode with an electron energy of 70 eV.

RESULTS

Apo-PHS was prepared by gel filtration of native enzyme in the presence of glutathione and deoxycholate (38). This produces protein in high yield which contains less than 1% of the original heme. The final specific activities of the protein used for the present experiments ranged from 27 to 87,000 units/mg protein. These values are lower than the values for the protein used by Kulmacz *et al.* (30) (88–125,000 units/mg) although the assay conditions are different; the specific activity of the protein used by Karthein *et al.* (23) was not stated.

Reaction of PPHP with Fe-PHS—When the organic hydroperoxide PPHP was added to Fe-PHS, a doublet ESR signal was observed at −196 °C after a 30-s incubation time at −12 °C (Fig. 1*A*). This doublet was centered at $g = 2.0036$ with a splitting of 21 gauss (peak to trough width, 33 gauss). At longer incubation times at −12 °C the spectrum changed irreversibly from a doublet to a singlet centered at the same *g* value with a peak to trough width of 30 gauss and poorly resolved hyperfine components (Fig. 1, *B* and *C*).

Reaction of Arachidonic Acid with Fe-PHS—Analysis of a reaction mixture at −196 °C immediately after addition of arachidonic acid demonstrated the presence of a doublet. The initial doublet observed at short incubation times (Fig. 2, *A* and *B*) was qualitatively similar in properties to the doublet

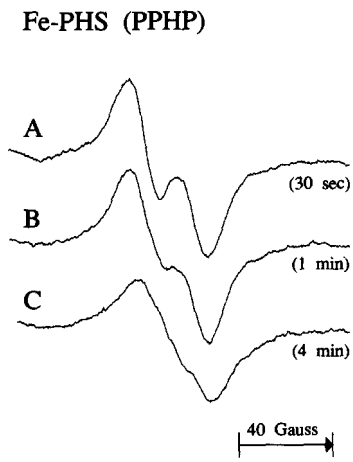

FIG. 1. **ESR spectra of Fe-PHS observed after different reaction times with PPHP.** Fe-PHS (50 μM) was incubated with 300 μM PPHP at −12 °C for various times and the spectra recorded at −196 °C at 2 mW and 4 gauss modulation amplitude as described in more detail under "Experimental Procedures." *A*, 30 s; *B*, 1 min; *C*, 4 min.

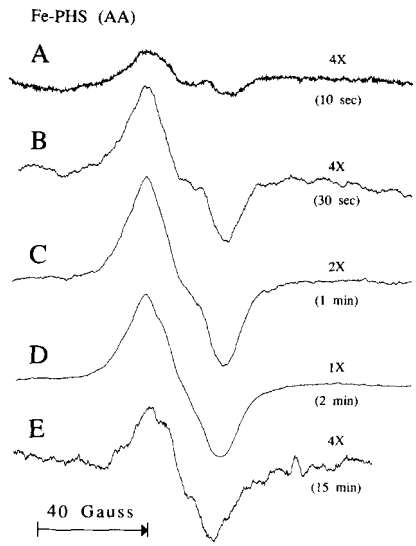

FIG. 2. **ESR spectra of Fe-PHS observed after different reaction times with arachidonic acid (*AA*).** Fe-PHS (75 μM) was incubated with 5 mM arachidonic acid at −12 °C at various times and the ESR spectra recorded at −196 °C. The details are described under "Experimental Procedures." The following conditions were used: microwave power, 2 mW; modulation amplitude, 8 gauss for *A*, 4 gauss for *B*, *C*, and *D*, with the relative gain indicated as × times. For *E* the spectrum was recorded at 22 °C after 15 min reaction of Fe-PHS at −12 °C and annealing the sample to 22 °C for 15 min (20 mW, 2 gauss; the reported spectrum in *E* was an accumulation of nine spectra; 17-mm flat cell). *A*, 10 s; *B*, 30 s; *C*, 1 min; *D*, 2 min; *E*, 15 min.

observed with PPHP (Fig. 1*B*) with a $g = 2.0042$, a splitting of 18 gauss, and a peak to trough width of 30 gauss. At longer incubation times at −12 °C the spectrum changed irreversibly to a singlet centered at the same g value, with nearly the same trough width and poorly resolved hyperfine splitting (Fig. 2, *C* and *D*). The singlet signal was rather stable at −12 °C and, in fact, was detected by recording the ESR spectrum at room temperature (Fig. 2*E*). The singlet spectral parameters recorded at 25 °C were similar to those recorded at −196 °C. This singlet was spectrally similar to the singlet recorded after the addition of PPHP to Fe-PHS. The doublet observed at early incubation times with arachidonic acid is not a one-component spectrum, but a sum of two spectra: a doublet similar to that formed by reaction with PPHP at the shortest incubation times, and the thermodynamically more stable singlet formed at longer incubation times. Neither the doublet nor the singlet was detected when the enzyme was treated with 200 μM indomethacin before the addition of arachidonic acid or when heat-denatured PHS was substituted for native enzyme. Addition of 200 μM indomethacin after the addition of arachidonic acid did not change the appearance of the singlet (data not shown).

Reaction of Arachidonic Acid with Mn-PHS—When arachidonic acid was added to Mn-PHS at −12 °C, there was a delay of 1 min before any radical signals were detected. The earliest detectable ESR signal was a very weak singlet (Fig. 3, *A* and *B*). After 3 min a broad singlet was detected with a g value centered at 2.0042 with a 31-gauss peak to trough width, and poorly resolved hyperfine structure (Fig. 3, *C* and *D*). Although the line shape of this singlet was similar to that observed with Fe-PHS, the hyperfine splitting was larger, and additional shoulders were detectable in the wings. The doublet signal seen at short times after the addition of arachidonic acid to Fe-PHS was not observed with Mn-PHS. Pretreatment of Mn-PHS with 200 μM indomethacin inhibited formation of the broad singlet at all reaction times.

To improve the resolution of the protein-derived radical formed with the Mn-PHS, the ESR spectra were recorded at various temperatures. At elevated temperatures, the resolution of the spectra was greatly improved, as seen in Fig. 3*E*. This radical was stable up to −73 °C, but noticeable decay was observed at −53 °C. Attempts to detect the Mn-PHS radical at room temperature, which was possible with the Fe-PHS-derived radical, were unsuccessful.

Reaction of PPHP with Mn-PHS—Addition of PPHP to Mn-PHS at −12 °C did not give rise to any detectable ESR signals at reaction times from 15 s to 15 min (Fig. 4, *A*, *B*, and *C*).

Characterization of Different Radical Species—Fig. 5 displays the microwave power saturation behavior at −196 °C of the three different radical species described above: the Fe-PHS doublet, the Fe-PHS singlet, and the Mn-PHS singlet. The singlet and doublet radicals formed by reaction with Fe-

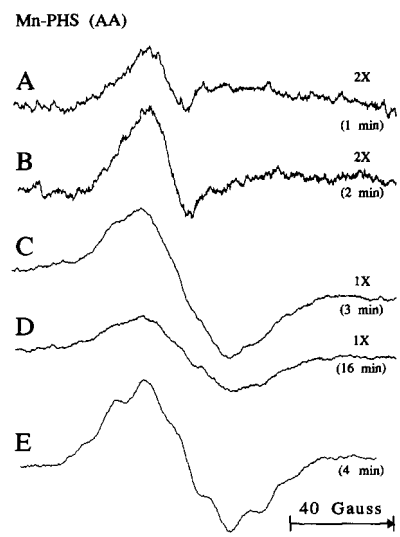

FIG. 3. **ESR spectra of Mn-PHS observed after different reaction times with arachidonic acid (*AA*).** Mn-PHS (75 μM) was incubated with arachidonic acid (5 mM) at −12 °C and the spectra recorded at −196 °C at 2 mW and 8-gauss modulation amplitude. *A*, 1 min; *B*, 2 min; *C*, 3 min; *D*, 16 min; *E*, ESR spectrum of Mn-PHS (50 μM) after a 4-min reaction with arachidonic acid (5 mM) at −12 °C but recorded at −73 °C (2 mW, 4 gauss).

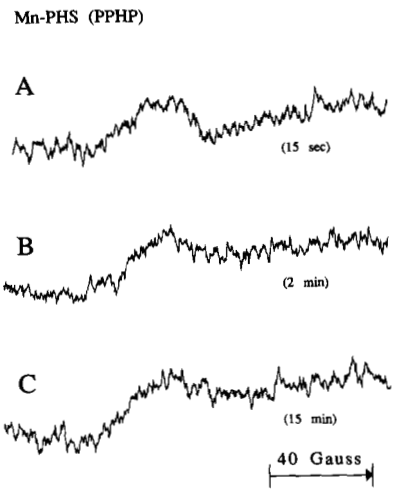

FIG. 4. **ESR spectra of Mn-PHS observed after different reaction times with PPHP.** Mn-PHS (50 μM) was incubated with 300 μM PPHP at −12 °C for various times and spectra recorded at −196 °C (2 mW; 4-gauss modulation amplitude). *A*, 15 s; *B*, 2 min; *C*, 15 min.

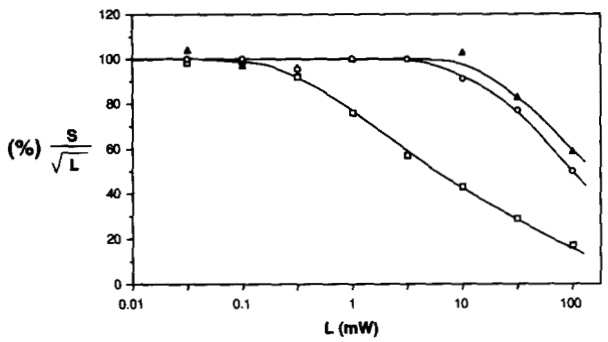

FIG. 5. **Microwave saturation at −196 °C of PHS-derived protein radicals.** *S*, ESR signal amplitude; *L*, microwave power. ▲, arachidonic acid doublet (Fe-PHS + arachidonic acid, 30-s incubation at −12 °C); ○, Fe singlet (Fe-PHS + arachidonic acid, 8-min incubation at −12 °C); □, Mn singlet (Mn-PHS + arachidonic acid, 4 min at −12 °C).

PHS exhibited very similar saturation behavior. For both, half-saturation occurred at 100 mW, showing a considerable magnetic interaction of the tyrosyl radicals with the nearby paramagnetic heme iron. The broad singlet produced by reaction of Mn-PHS with arachidonic acid exhibited half-saturation at 5 mW.

The two doublets formed by reaction of Fe-PHS with arachidonic acid and PPHP, respectively, revealed striking similarities with spectra of protein-derived tyrosyl radicals in ribonucleotide reductase from *Escherichia coli* as well as from the mammalian enzyme (25, 42–44). Recently, Tyr^{122} was identified as the radical site in *E. coli* ribonucleotide reductase by x-ray crystallography (24). Karthein *et al.* (22) proposed that the doublet spectrum in Fe-PHS originates from tyrosyl radicals. The hyperfine data for the tyrosyl radicals of ribonucleotide reductase were determined with high spectral resolution by electron nuclear double resonance (45). Single crystal ESR was performed on an irradiated sample of L-tyrosine HCl by Fasanella and Gordy (46). The best simulation of the doublet spectrum formed by reaction of PPHP with Fe-PHS is shown in Fig. 6. The hyperfine coupling constants are closer to those of irradiated L-tyrosine HCl but still similar to those of the tyrosyl radical of ribonucleotide reductase (Table I). Whereas the dihedral angle between the

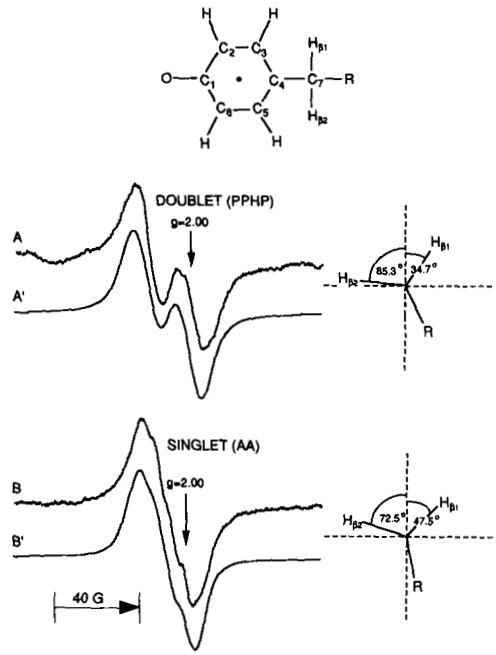

FIG. 6. **ESR line shape of protein-derived tyrosyl radicals (at −196 °C) in Fe-PHS and corresponding dihedral angles of the conformation of methylene protons (pi-orbital axis is *vertical*).** *A*, doublet signal formed in Fe-PHS after 10-s reaction with PPHP at −12 °C; *B*, singlet signal formed in Fe-PHS after 2-min reaction with arachidonic acid (*AA*) at −12 °C. *A'* and *B'* are the corresponding computer simulations using the data reported in Table I with Lorentzian line widths of 6- and 4.2-gauss, respectively.

TABLE I

Magnetic parameters of tyrosyl radicals in Fe-PHS

All hyperfine coupling constants are given in units of gauss, and α is the first Euler rotation angle.

Nuclei	Parameter	Singlet[a] (AA)	Doublet (AA)	Doublet[b] (PGG_2)
	g_x	2.0067	2.0067	2.0080
	g_y	2.0045	2.0045	2.0030
	g_z	2.0020	2.0020	2.0030
	g_{iso}			
$H(C_2)$	A_x	−3.1	−3.1	−3.5
	A_y	−9.0	−9.0	−8.5
	A_z	−6.5	−6.5	−5.0
	a_{iso}	−6.2	−6.2	−5.6
	α	+60°	+60°	
$H(C_6)$	A_x	−3.0	−3.0	−3.5
	A_y	−9.0	−9.0	−8.5
	A_z	−6.5	−6.5	−5.0
	a_{iso}	−6.2	−6.2	−5.6
	α	−60°	−60°	
$H(\beta_1)$	a_{iso}	+12.3	+18.2	+18.0
	θ	+47.5°	+34.7°	
$H(\beta_2)$	a_{iso}	+2.5	+0.2	+6.0
	θ	−72.5°	−85.3°	

[a] AA, arachidonic acid.
[b] From Ref. 22.

strongly coupled methylene hydrogen and the pi-orbital axis is 30° in ribonucleotide reductase, the dihedral angle is 34.7° in Fe-PHS.

The line shape of the poorly resolved singlet formed in Fe-PHS after longer reaction times with arachidonic acid or PPHP appears similar to the ESR spectra of tyrosyl radicals detected in photosystem II and tyrosyl radicals in oxidized

metmyoglobin (47–49). We assumed that the singlet in Fe-PHS also originated from tyrosyl radicals and used a large hyperfine coupling constant for the strongly coupled methylene proton consistent with a larger theta angle for simulation of the ESR spectrum. The best simulation yielded a tyrosyl radical with a dihedral angle of 47.5° for this methylene proton (Table I; Fig. 6). The saturation behavior for the Fe-PHS doublet and singlet is nearly identical (half-saturation, 100 mW) implying a short distance interaction with the iron. Both singlet and doublet tyrosyl radical signals may arise from the same tyrosine residue of the enzyme, and the differences in spectral appearance may be caused by an irreversible conformational change at longer reaction times.

The broad singlet appearing in Mn-PHS after approximately a 4-min reaction with arachidonic acid exhibited a larger separation of the partially resolved hyperfine coupling constants (11 gauss instead of 6.5 gauss for the singlet in Fe-PHS) and shoulders in the wings and is *inconsistent* with any tyrosyl radical structure. The ESR spectrum recorded at −73 °C shows improved resolution (Fig. 3*E*); the second derivative exhibits a nearly symmetric septet of lines (data not shown). From the ESR spectral data we conclude that the radical species found in Mn-PHS is not a tyrosyl radical.

During the oxidation of arachidonic acid by Fe-PHS a change of spin state of the heme iron from high spin to low spin was observed by ESR (22). We looked for analogous changes at the manganese center in enzyme reconstituted with Mn(III)-protoporphyrin IX. Unfortunately, neither in untreated Mn-PHS nor after the addition of arachidonic acid were any high spin or low spin ESR signals from manganese detected between 600 and 3,400 gauss at −196 °C (39 mW, 10-gauss modulation) as well as from 0–4,000 gauss (100 mW, 5-gauss modulation) at 4.2 K (data not shown).

Kinetics of Formation and Decay of the Radicals—After the initial ESR spectra were recorded at −196 °C, the sample tubes were warmed to −12 °C and allowed to incubate for an additional period of time. The tubes were then refrozen and another spectrum recorded at −196 °C. By sequentially repeating this procedure, it was possible to determine an approximate time course for the formation and decay of the radical signals. At the earliest time point after the addition of arachidonic acid to Fe-PHS, the doublet dominated over the singlet (Fig. 7). The integral intensity increased sharply, reaching a maximum of approximately 5 μM at 45–120 s in different experiments. The doublet signal decayed rapidly so that at 3 min the singlet was the only detectable signal. The singlet persisted for up to 16 min.

Fig. 8 demonstrates that the doublet was the predominant ESR signal detected 10 s after the addition of PPHP to Fe-PHS. The integral intensity was maximal at this time point and corresponded to a radical concentration of 8 μM. The singlet signal appeared rapidly but persisted as was observed in the reactions with arachidonic acid and Fe-PHS.

Fig. 9 displays the time course of radical formation after the addition of arachidonic acid to Mn-PHS. At short times, very low radical levels were detectable. After a lag period of 3 min, a detectable radical was observed, and by 5–7 min the radical concentration had increased to 8 μM. The intensity of the radical signal decreased slowly with time but more rapidly than in the case of the Fe-PHS-derived radicals. As described earlier, no trace of the doublet signal was detectable at any time.

Effect of Phenol on Radical Formation—The fact that no radicals could be detected after the addition of PPHP to Mn-PHS suggested an important role for the peroxidase in radical generation. To explore this further, incubations were carried out with arachidonic acid and PPHP in the presence of phenol, a reducing substrate for the peroxidase (50). Such agents reduce compound I to compound II and then compound II to resting enzyme. If tyrosyl radical formation requires protein oxidation by a ferryl form of the enzyme, one anticipates that phenol would prevent radical formation by reducing these ferryl derivatives. Fig. 10 displays the ESR spectrum recorded at −196 °C after incubation of Fe-PHS and arachidonic acid for 10 s at −12 °C in the presence of 50 μM phenol. The major signal detected was the singlet, which was similar in appearance to the singlet detected in the absence of phenol

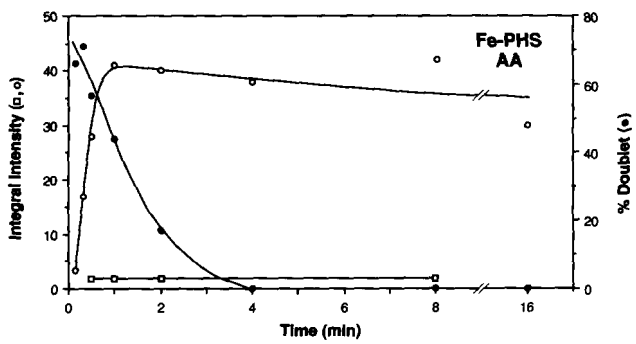

FIG. 7. **Kinetics for the formation and conversion of tyrosyl radicals appearing after addition of arachidonic acid (*AA*) to Fe-PHS.** Arachidonic acid (5 mM) was incubated with Fe-PHS (50 μM) at −12 °C and the ESR spectra recorded at −196 °C at various times after the addition of arachidonic acid as described under "Experimental Procedures." ○, integral intensity of ESR spectra (doublet + singlet); ●, percentage of doublet signal; □, heat-denatured Fe-PHS and arachidonic acid.

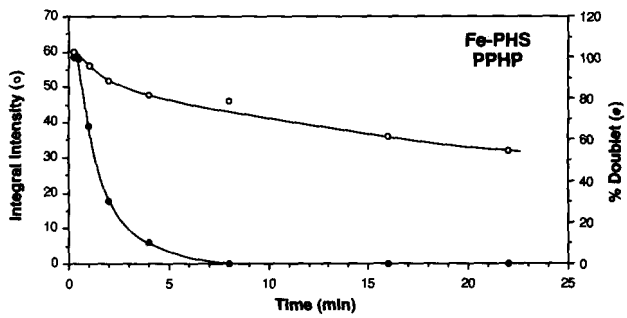

FIG. 8. **Kinetics of the formation and conversion of tyrosyl radicals appearing after addition of PPHP to Fe-PHS.** PPHP (300 μM) was incubated with Fe-PHS (50 μM) at −12 °C and the ESR spectra recorded at −196 °C at various times after the addition of the PPHP. ○, integral intensity of ESR spectra (doublet + singlet); ●, percentage of doublet signal.

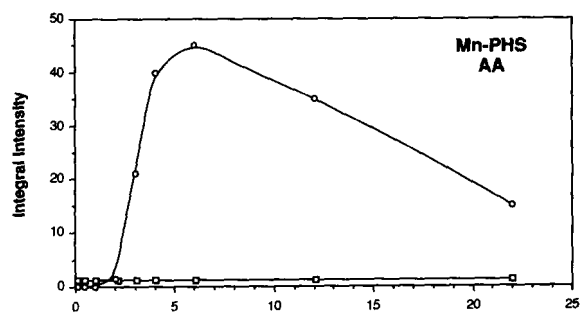

FIG. 9. **Kinetics of the formation and decay of radicals appearing after the reaction of Mn-PHS with arachidonic acid (*AA*).** Arachidonic acid (5 mM) was incubated with Mn-PHS (50 μM) at −12 °C and the ESR spectra recorded at −196 °C. ○, control; □, preincubated with indomethacin.

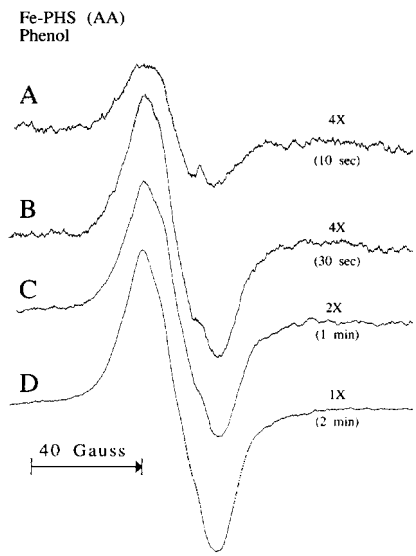

FIG. 10. **ESR spectra obtained by incubating Fe-PHS after different reaction times with arachidonic acid (*AA*) in presence of phenol.** Fe-PHS (50 μM) was incubated with arachidonic acid (5 mM) in the presence of phenol (50 μM) at −12 °C and the spectra recorded at −196 °C after the addition of arachidonic acid. Spectra were recorded at 2 mW and 4-gauss modulation amplitude. *A*, 10 s; *B*, 30 s; *C*, 1 min; *D*, 2 min.

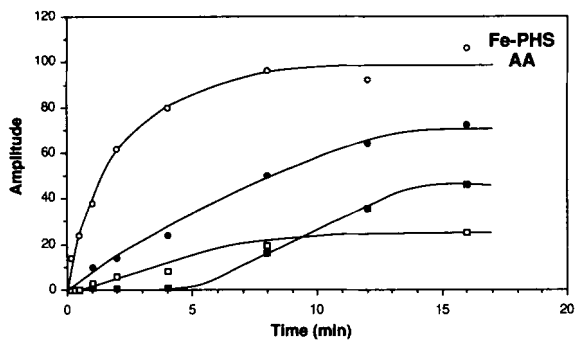

FIG. 11. **Kinetics of the formation and decay of tyrosyl radicals observed on incubation of Fe-PHS with arachidonic acid (*AA*) in presence of phenol and indomethacin.** Fe-PHS (50 μM) was incubated with arachidonic acid (5 mM) at −12 °C and the spectra recorded at −196 °C at times after the addition of arachidonic acid. Phenol and indomethacin were added prior to the addition of arachidonic acid. ○, control; ●, phenol (50 μM); □, phenol (500 μM); ■, indomethacin (100 μM). Spectra intensities are reported as relative amplitudes.

after longer incubation times. No significant doublet ESR signal was detected at any time after the addition of arachidonic acid. The presence of 50 μM phenol also lowered the intensity of the singlet at all times examined (Fig. 11). Further diminution of radical signal was apparent when incubations were carried out in the presence of 500 μM phenol.

Inclusion of 50 μM phenol in reactions of Fe-PHS with 300 μM PPHP decreased the initial concentration of tyrosyl radicals 4-fold compared with incubations without phenol (Fig. 12). No change in the extent of protein-derived radical formation was observed when incubations were carried out with Mn-PHS and arachidonic acid in the presence of 50 μM phenol. Neither the rate nor the extent of formation of the broad singlet was affected by the presence of phenol (Fig. 13).

Effect of Indomethacin on Radical Formation—The influence of preincubation with the cyclooxygenase inhibitor indomethacin on the formation of radicals in Fe-PHS and Mn-PHS was followed for short and long reaction times with

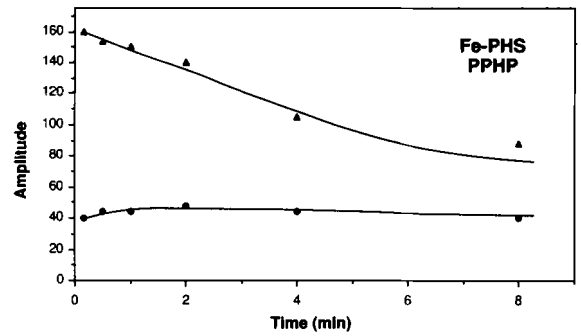

FIG. 12. **Kinetics for the formation and decay of tyrosyl radicals by Fe-PHS with PPHP in presence of phenol.** Fe-PHS (50 μM) was incubated at −12 °C with PPHP (300 μM) in the presence of phenol (50 μM). Spectra were recorded at −196 °C, and the intensities are reported as relative amplitudes. Phenol was added prior to the addition of the PPHP. ▲, control; ●, phenol (50 μM).

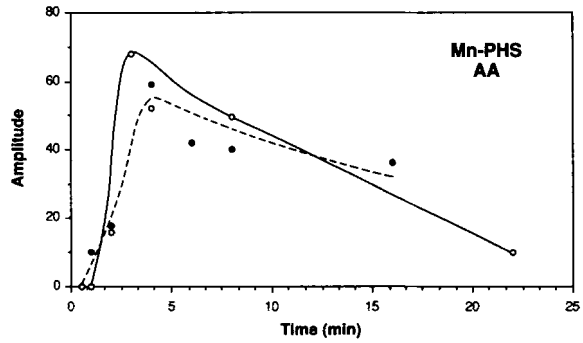

FIG. 13. **Kinetics for formation and decay of radicals by Mn-PHS incubated with arachidonic acid (*AA*) in presence of phenol.** Mn-PHS (50 μM) was incubated with arachidonic acid (5 mM) at −12 °C in the presence of 50 μM phenol. Spectra were recorded at −196 °C at times after the addition of arachidonic acid, and the spectral intensities are reported as relative ESR amplitudes. ○ and *solid line*, control; ● and *dashed line*, phenol (50 μM).

arachidonic acid. In Fe-PHS having cyclooxygenase and peroxidase activity, neither the doublet nor the singlet was observed between 10 s and 5 min reaction time with arachidonic acid after incubation with 100 μM indomethacin. However, after 7 min of incubation the singlet was detected and gradually increased to nearly 50% of the control (Fig. 11). With Mn-PHS, which has cyclooxygenase but not peroxidase activity, the broad singlet did not appear at any time after incubation of the enzyme with 100 μM indomethacin (Fig. 9).

Low Temperature Metabolism of Arachidonic Acid—The metabolism of arachidonic acid was studied utilizing the conditions employed in the ESR studies. The arachidonic acid metabolite profile was revealed by HPLC analysis. A typical profile obtained from incubations with Fe-PHS and Mn-PHS is shown in Fig. 14. Four predominant metabolites were observed in incubations at −12 °C. The peaks at 18 and 21 min coeluted with PGE_2 and 15-hydroperoxy-PGE_2, the decomposition products of PGG_2 and PGH_2. The major metabolite (60 min) coeluted with 12-hydroxyheptadecatrienoic acid, which is also a decomposition product of PGH_2. The formation of additional metabolites was indicated by the presence of peaks that eluted at approximately 70 min, a region where HETEs elute. In addition, the formation of polar metabolites of arachidonic acid, which eluted at the solvent front, was noted (particularly from incubations with Fe-PHS). As can be seen in Fig. 14, PGE_2 and 15-hydroperoxy-PGE_2 were not the principal decomposition products of PGG_2 and PGH_2 under these incubation conditions. 12-Hydroxyhepta-

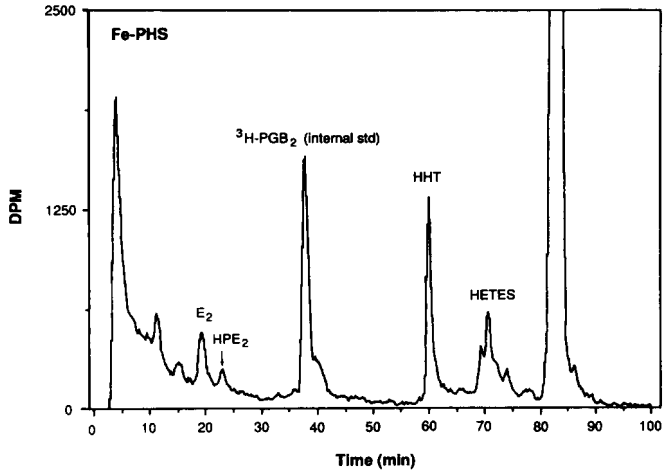

FIG. 14. **Separation of arachidonic acid metabolites formed by PHS at −12 °C.** Fe-PHS (50 μM) was incubated with [^{3}H] arachidonic acid (5 mM) at −12 °C for 10 min. The sample was extracted and the eicosanoids separated by HPLC analysis as described under "Experimental Procedures." *HP*, hydroperoxy; *HHT*, 12-hydroxyheptadecatrienoic acid.

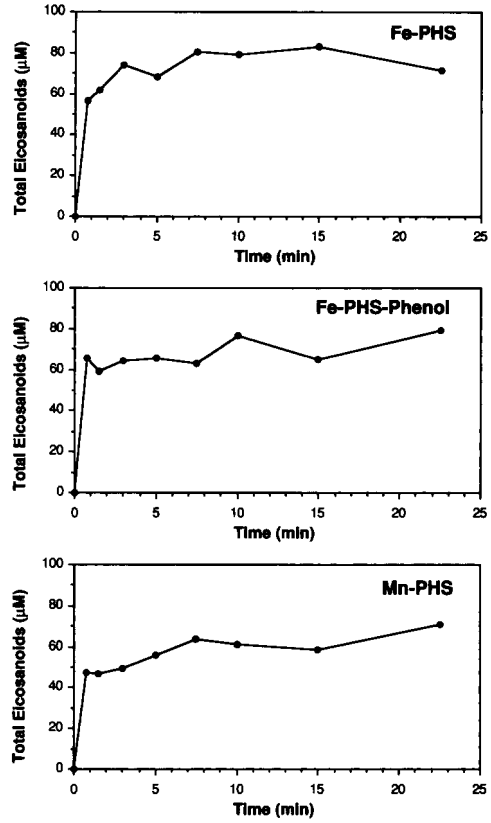

FIG. 15. **Kinetics of formation of eicosanoids by PHS at −12 °C as estimated by HPLC analysis.** PHS (50 μM) was incubated with radiolabeled arachidonic acid (5 mM) at −12 °C and aliquots removed at various times and analyzed after extraction by HPLC. Samples were corrected for recovery by the use of an internal standard and converted to mass units. *A*, Fe-PHS; *B*, Fe-PHS in the presence of 50 μM phenol; *C*, Mn-PHS.

decatrienoic acid appears to be the major decomposition product.

Preparative scale incubations were performed, and the unidentified metabolites eluting at 60 and 70 min were isolated. On-line UV analysis revealed both peaks to have absorbance maxima at 235 nm, indicative of a diene structure. These metabolites were then derivatized and analyzed by GC/MS. The peak eluting at 60 min on HPLC and tentatively identified as 12-hydroxyheptadecatrienoic acid yielded diagnostic ions at *m/z* 173 and 301, which confirms the identification as 12-hydroxyheptadecatrienoic acid. The peak eluting at 70 min on HPLC was resolved into two components by GC/MS. The first of these components, which constituted about 75% of the total mass, yielded diagnostic ions at *m/z* 229 and 287 and was identified as 11-HETE. The second component yielded diagnostic ions at *m/z* 173 and 343 and was identified as 15-HETE. Thus, in addition to the formation of prostaglandins, both 11-HETE and 15-HETE were formed by PHS under these incubation conditions.

The kinetics of low temperature metabolism of arachidonic acid for both Fe-PHS and Mn-PHS under conditions identical to those used for ESR studies are depicted in Fig. 15. As can be seen by viewing Fig. 15, the formation of prostaglandins was very rapid and was essentially complete within 1 min after the addition of arachidonic acid for both Fe-PHS and Mn-PHS. This rapid rate of prostaglandin formation and inactivation of PHS is similar to what is seen for PHS at 37 °C with lower enzyme and arachidonic acid concentrations. The addition of phenol to incubations containing Fe-PHS did not increase the level of metabolism. Approximately 60–80 μM eicosanoids were formed with 50 μM Fe-PHS or Mn-PHS.

To investigate the possibility that high enzyme and substrate concentrations and possible oxygen depletion could be altering the behavior of the enzyme, low temperature kinetics were also studied at lower concentrations of enzyme and substrate (data not shown). By using 2.5 μM Fe-PHS/Mn-PHS and 100 μM arachidonic acid, metabolism profiles were obtained similar to those shown in Fig. 14. In addition, the time course for arachidonic acid metabolism was the same as in the high enzyme concentration metabolism experiment. Addition of 500 μM phenol to incubations containing 2.5 μM Fe-PHS did not increase metabolite formation or alter the distribution of products.

DISCUSSION

Radical Production by PHS—ESR spectroscopy has been used previously to explore the mechanism of arachidonic acid oxidation by microsomal or purified PHS. Egan *et al.* (51) reported that addition of arachidonic acid or PGG_2 to sheep seminal vesicle microsomes gives rise to a featureless radical signal with a *g* value around 2.0 which is detectable at −196 °C after rapid freezing (from 25 °C). Kalyanaraman *et al.* (32) demonstrated that this radical was most likely protein derived. Kulmacz *et al.* (31) reported the formation of a doublet ESR signal at $g = 2.0003$ with 22 gauss splitting and 40 gauss peak-to-trough width after the reaction of H_2O_2 with purified PHS. They did not propose a structure for this radical, but its spectral properties are very similar to those later assigned to a tyrosyl radical by Karthein *et al.* (22). Karthein *et al.* demonstrated that the doublet is formed in incubations of PHS with arachidonic acid or PGG_2 and that it is short lived even at −12 °C. Kulmacz *et al.* (30) analyzed the hyperfine structure of the singlet formed after the reaction of Fe-PHS with a hydroperoxide and assigned its structure as a tyrosyl radical with an altered conformation relative to the doublet.

The radicals detected in the present study in incubations of arachidonic acid or PPHP with Fe-PHS exhibited spectral properties similar to those of the tyrosyl radicals reported by Karthein *et al.* (22) and Kulmacz *et al.* (30) (Table I). The maximal radical yields corresponded to ~10% of the protein molecules for Fe-PHS and 17% of the protein molecules for Mn-PHS. These values are lower than the values reported by Karthein *et al.* (~35% for Fe-PHS), which may reflect differ-

ences in specific activity, heme content, etc.

As outlined in Fig. 6 and Table I, two types of tyrosyl radicals with different dihedral angles (32° and 47.5°) for the methylene protons were observed and characterized for Fe-PHS. The first was observed as a doublet whereas the one with the larger dihedral angle appeared as a singlet. A doublet tyrosyl radical signal is present in ribonucleotide reductase (25, 43, 44) whereas a singlet tyrosyl radical signal is observed in photosystem II (48). Thus, Fe-PHS exhibits both types of tyrosyl radicals and conversions or transitions between them. In Fe-PHS, the doublet converts irreversibly into the singlet at longer reaction time. Both signals have nearly identical saturation behavior (Fig. 5) and on this basis are probably caused by a radical on the same tyrosine residue in the enzyme. The doublet to singlet transition may result from a protein conformational change that twists the methylene group at the tyrosine site. An alternate explanation is that the transformation of the doublet to the singlet results from reduction of the doublet tyrosyl radical by another tyrosine residue. These different tyrosyl radicals would have to be located similar distances from the iron to explain their similar power saturation behavior.

Although Mn-PHS exhibits cyclooxygenase activity, the type of radicals and the kinetics of their formation and decay are completely different from the iron enzyme. Doublet and singlet signals from tyrosyl radicals do not appear in Mn-PHS. The broad singlet with the incompletely resolved septet pattern was unlike any ESR spectrum from a tyrosyl radical reported previously. The Mn-PHS protein-derived radical was much easier to saturate than either type of tyrosyl radical in Fe-PHS, and it had a shorter lifetime than the singlet in Fe-PHS.

Mn-PHS has a similar stoichiometry of prosthetic group binding to protein, similar resistance to cleavage at Arg^{277} by trypsin, similar sensitivity to acetylation by aspirin, but somewhat diminished sensitivity to oxidative autoinactivation (as a result of its low peroxidase activity) (11, 52, 53). Thus, although it is likely that structural differences exist between Mn-PHS and Fe-PHS, their gross structures appear similar. On a superficial level then, it seems surprising that different amino acid residues would be oxidized by these structurally similar proteins. Here, cytochrome *c* peroxidase provides a useful precedent. Oxidation of native cytochrome *c* peroxidase by H_2O_2 produces a tryptophanyl radical along with a minor component that appears to be a tyrosyl radical. As expected, mutation of Trp^{191} to phenylalanine abolishes formation of the tryptophanyl radical and increases the yield of the tyrosyl radical (54). However, the ability of enzyme to form the tryptophanyl radical is also abolished by mutation of Asp^{235} to asparagine (54). Asp^{235} is hydrogen-bonded to the indole N of Trp^{191}, and loss of this hydrogen bond in the mutant protein causes a 180° rotation of the tryptophan side chain. This subtle conformational change apparently diminishes the ability of Trp^{191} to be oxidized by the ferryl derivative of the heme center. In this mutant enzyme, protein-derived radicals appear to derive from tyrosine residues. Thus, subtle changes in local environment can alter the identity of protein groups oxidized by the heme center. The fact that Mn-PHS does not form tyrosyl radicals but exhibits cyclooxygenase activity suggests that the tyrosyl radicals detected in incubations with Fe-PHS are not important for cyclooxygenase catalysis.

Role of the Peroxidase in Radical Generation—Several lines of evidence suggest that production of tyrosyl radicals after the addition of arachidonic acid or PPHP to Fe-PHS is dependent on the peroxidase reaction. 1) Addition of PPHP to Mn-PHS does not produce any detectable protein radical signals consistent with the very low peroxidase activity of the mangano enzyme. 2) Indomethacin, a potent cyclooxygenase inhibitor, prevents formation of tyrosyl radicals in the reaction of Fe-PHS with arachidonic acid. 3) Inclusion of 1 equivalent of the peroxidase reducing substrate phenol in incubations of 1 equivalent Fe-PGH synthase and 100 equivalents arachidonic acid completely abolishes formation of the doublet tyrosyl radical and decreases the concentration of the singlet tyrosyl radical by 35%. Increasing the phenol concentration to 10 equivalents further decreases the concentration of singlet tyrosyl radical by 70% relative to the no-phenol control. The ability of phenol to attenuate radical production is caused by reduction of the peroxidase higher oxidation states; addition of phenol to the preformed radicals leads to no reduction (data not shown). Likewise, the presence of phenol in reactions of arachidonic acid and Mn-PHS does not diminish the intensity of the broad singlet radical signal. Thus, phenol attenuation of radical signals requires the presence of an efficient peroxidase activity.

Although indomethacin inhibited tyrosyl radical formation in reactions of arachidonic acid and Fe-PHS, the singlet tyrosyl radical signal was observed after prolonged incubations. Because the cyclooxygenase activity was nearly completely inhibited under these conditions, we attribute formation of this radical signal to nonenzymatic oxidation of arachidonic acid to hydroperoxides that react with the peroxidase of Fe-PHS to generate the singlet tyrosyl radical. Indomethacin does not inhibit the peroxidase reaction so its presence would not inhibit protein oxidation by the peroxidase. However, incomplete inhibition of the cyclooxygenase would also account for the finding. Kulmacz *et al.* (30) reported that incubation of ethyl hydroperoxide with indomethacin-inhibited Fe-PHS produces a singlet tyrosyl radical signal but not a doublet, in line with the present observations. The importance of the peroxidase activity for the generation of the singlet on prolonged incubation of arachidonic acid with indomethacin-inhibited Fe-PHS is suggested by the observation that similar incubations with Mn-PHS do not produce any detectable radicals even after long times.

The production of a radical signal by reaction of arachidonic acid with Mn-PHS indicates that there is a peroxidase-independent pathway for radical generation (Scheme 2). The oxidizing agent that produces the singlet radical signal is uncertain but may be an oxidized derivative of arachidonic acid. The currently accepted mechanism for the cyclooxygenase reaction involves peroxyl radical derivatives of arachidonic acid as intermediates (16, 17). Peroxyl radicals are well known oxidizing agents so it is conceivable that such a substrate derivative oxidizes a protein residue on PHS (55).

Significance of Radical Production—Several lines of evidence question the role of the protein-derived radicals as

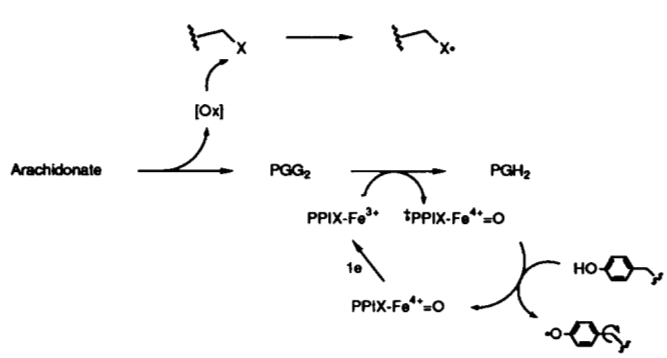

SCHEME 2. **Pathways for oxidation of PHS protein residues during catalytic turnover.**

catalytically competent intermediates in the synthesis of prostaglandins by PHS. The most compelling finding was obtained from a comparison of the temporal relationship between the formation of the protein-derived radicals and the formation of arachidonic acid metabolites by both Fe-PHS and Mn-PHS. Analysis of the arachidonic acid metabolites produced by the enzyme at −12 °C under identical conditions used for ESR studies produced several unexpected results. In addition to prostaglandins, both 11-HETE (major) and 15-HETE (minor) were formed in significant quantities by the enzyme. These metabolites have been detected previously, but their abundance in the present experiments (especially 11-HETE) may indicate that at −12 °C the reaction depicted in Equation 1 between the carbon-centered radical intermediates and molecular oxygen occurs without closure to the five-membered ring (56). The formation of eicosanoids commmenced immediately after the addition of [^{3}H]arachidonic acid to Fe-PHS and Mn-PHS and at the earliest time point that could be measured (45 s) was near maximal levels. This rate of arachidonic acid oxygenation is very similar to what is observed in incubations at 37 °C. In contrast, the doublet and the singlet formed by the reaction of arachidonic acid with Fe-PHS appeared to be formed at a slower rate. The doublet tyrosyl radical appeared to be a transient precursor to the singlet tyrosyl radical. Although the formation of the singlet ESR signal is maximal by 1 min under these conditions, its level decreased only 20% by 15 min, long after arachidonic acid oxygenation had stopped. A more dramatic discrepancy between protein-derived radical formation and cyclooxygenase activity is observed with Mn-PHS. The initial rate of arachidonic acid oxygenation to eicosanoids by Mn-PHS is also very rapid and commences immediately after the addition of arachidonic acid to the enzyme at −12 °C. The formation of eicosanoids is essentially complete by 1 min of incubation. In contrast, the broader protein-derived radical formed by Mn-PHS is not detectable until 3 min, reaches maximal levels by 5 min, then declines in an apparent zero order fashion by 70% over the next 17 min. The comparison of the time course of arachidonic acid oxygenation and protein-derived radical formation suggests that the radicals are not catalytically competent intermediates of cyclooxygenase catalysis with either Fe-PHS or Mn-PHS. The protein-derived radicals appeared to be formed during or after the formation of the eicosanoids.

The addition of the peroxidase substrate, phenol, significantly inhibited the formation of the tyrosyl doublet and suppressed the tyrosyl singlet observed with the Fe-PHS on incubation with either arachidonic acid or PPHP. Phenol did not alter the formation of the non-tyrosyl radical produced by Mn-PHS. This reinforces the hypothesis that the formation of tyrosyl radicals by Fe-PHS is a result of its peroxidase activity. Phenol could reduce the higher oxidation states of the heme prosthetic group before they can oxidize tyrosine residues on the protein.

The addition of phenol did not alter the rate of eicosanoid formation by either Fe-PHS or Mn-PHS. If the spectrally detectable tyrosyl radicals were intermediates in cyclooxygenase catalysis, one would anticipate that prevention of their formation by the addition of phenol would inhibit cyclooxygenase activity. This was not observed, which further supports the conclusion that the protein-derived radicals are not intermediates in cyclooxygenase catalysis.

Finally, the observation that Mn-PHS, which has only cyclooxygenase but not peroxidase activity, apparently does not form tyrosyl radicals at all strongly suggests that tyrosyl radicals are not required for cyclooxygenase activity.

What then is the significance of radical production? The present observations correlate rather well with previous studies of the autoinactivation of PHS (29, 50, 57, 58). Fe-PHS undergoes arachidonic acid- and hydroperoxide-dependent inactivation that is attenuated to some extent by the presence of peroxidase-reducing substrates (29, 50, 53, 58). Mn-PHS is less sensitive to autoinactivation but still loses catalytic activity irreversibly in the presence of arachidonic acid (53). This implies that peroxidase-dependent and peroxidase-independent pathways for autoinactivation exist. The production of spectrally detectable, persistent tyrosyl radicals during PHS turnover may reflect oxidative modification of the protein. Previous studies have established that an important cause of PHS autoinactivation is protein oxidation (59), and we suggested that the formation of protein-derived radicals is associated with inactivation (32).

Although our studies do not support a role for *spectrally detectable* tyrosyl radicals in cyclooxygenase catalysis, they do not rule out the involvement of tyrosyl radicals or other protein-derived radicals in the catalytic cycle of the enyzme. Tyrosine residues are clearly important for catalytic activity as indicated by chemical modification and site-directed mutagensis experiments (33). Catalytically competent tyrosyl radicals may be generated and react with arachidonic acid on a time scale that prevents their detection by ESR spectroscopy. In fact, given the high rate of oxygenation of arachidonic acid by PHS, even at −12 °C, it seems likely that whatever group on the enzyme affects substrate oxidation will be present in low steady-state concentrations. Alternatively, tyrosine residues may be involved in the cyclooxygenase reaction but not in the form of tyrosyl radicals. Oxidation of such residues to tyrosyl radicals could then be viewed as an initial event leading to enzyme inactivation.

Acknowledgments—Measurements at 4.2 K were performed with a Varian E-9 spectrometer and a He gas flow cryostat at the Biomedical ESR Center of the Medical College of Wisconsin, Milwaukee in collaboration with Dr. W. Antholine. We also wish to thank Steve McGown for mass spectral analysis of eicosanoids.

REFERENCES

1. DeWitt, D. L., and Smith, W. L. (1988) *Proc. Natl. Acad. Sci. U. S. A.* **85,** 1412–1416
2. Hamberg, M., Svensson, J., Wakabayashi, T., and Samuelsson, B. (1974) *Proc. Natl. Acad. Sci. U. S. A.* **71,** 345–349
3. Nugteren, D. H., and Hazelhof, E. (1973) *Biochim. Biophys. Acta* **326,** 448–461
4. Pace-Asciak, C. R., and Smith, W. L. (1983) in *The Enzymes* (Boyer, P. D., ed) Vol. 16, pp. 544–603, Academic Press, New York
5. Merlie, J. P., Fagan, D., Mudd, J., and Needleman, P. (1988) *J. Biol. Chem.* **263,** 3550–3553
6. Yokoyama, C., Takai, T., and Tanabe, T. (1988) *FEBS Lett.* **231,** 347–351
7. DeWitt, D. L., El-Harith, E. A., Kraemer, S. A., Andrews, M. J., Yao, E. F., Armstrong, R. L., and Smith, W. L. (1990) *J. Biol. Chem.* **265,** 5192–5198
8. Van Der Ouderaa, F. J., Buytenhek, M., Nugteren, D. H., and Van Dorp, D. A. (1977) *Biochim. Biophys. Acta* **487,** 315–331
9. Van Der Ouderaa, F. J., Buytenhek, M., Slikkerveer, F. J., and Van Dorp, D. A. (1979) *Biochim. Biophys. Acta* **572,** 29–42
10. Roth, G. J., Machuga, E. T., and Strittmatter, P. (1981) *J. Biol. Chem.* **256,** 10018–10022
11. Kulmacz, R. J., and Lands, W. E. M. (1984) *J. Biol. Chem.* **259,** 6358–6363
12. Ohki, S., Ogino, N., Yamamoto, S., and Hayaishi, O. (1979) *J. Biol. Chem.* **254,** 829–836
13. Hamberg, M., and Samuelsson, B. (1967) *J. Biol. Chem.* **242,** 5336–5343
14. Mason, R. P., Kalyanaraman, B., Tainer, B. E., and Eling, T. E. (1980) *J. Biol. Chem.* **255,** 5019–5022
15. Schreiber, J., Eling, T. E., and Mason, R. P. (1986) *Arch. Biochem. Biophys.* **249,** 126–136

16. Porter, N. A., and Funk, M. O. (1975) *J. Org. Chem.* **40,** 3614–3615
17. Marnett, L. J., and Maddipati, K. R. (1991) in *Peroxidases in Chemistry and Biology* (Everse, J., Everse, K. E., and Grisham, M. B., eds) Vol. 1, pp. 293–334, CRC Press, Boca Raton, FL
18. Lambeir, A. M., Markey, C. M., Dunford, H. B., and Marnett, L. J. (1985) *J. Biol. Chem.* **260,** 14894–14896
19. Nastainczyk, W., Schuhn, D., and Ullrich, V. (1984) *Eur. J. Biochem.* **144,** 381–385
20. Hemler, M. E., and Lands, W. E. M. (1980) *J. Biol. Chem.* **255,** 6253–6261
21. Kulmacz, R. J., and Lands, W. E. M. (1983) *Prostaglandins* **25,** 531–540
22. Karthein, R., Dietz, R., Nastainczyk, W., and Ruf, H. H. (1988) *Eur. J. Biochem.* **171,** 313–320
23. Dietz, R., Nastainczyk, W., and Ruf, H. H. (1988) *Eur. J. Biochem.* **171,** 321–328
24. Nordlund, P., Sjöberg, B.-M., and Eklund, H. (1990) *Nature* **345,** 593–598
25. Sjöberg, B.-M., and Graslund, A. (1983) in *Advances in Inorganic Biochemistry* (Eichelhorn, G. L., Marcilli, L., and Theil, E. C., eds) p. 87, Elsevier Science Publishing Co., New York
26. Ogino, N., Ohki, S., Yamamoto, S., and Hayaishi, O. (1978) *J. Biol. Chem.* **253,** 5061–5068
27. Shimokawa, T., and Smith, W. L. (1991) *J. Biol. Chem.* **266,** 6168–6173
28. Marnett, L. J., Chen, Y.-N. P., Maddipati, K. R., Plé, P., and Labeque, R. (1988) *J. Biol. Chem.* **263,** 16532–16535
29. Raz, A., and Needleman, P. (1990) *Biochem. J.* **269,** 603–607
30. Kulmacz, R. J., Ren, Y., Tsai, A.-L., and Palmer, G. (1990) *Biochemistry* **29,** 8760–8771
31. Kulmacz, R. J., Tsai, A.-L., and Palmer, G. (1987) *J. Biol. Chem.* **262,** 10524–10531
32. Kalyanaraman, B., Mason, R. P., Tainer, B., and Eling, T. E. (1982) *J. Biol. Chem.* **257,** 4764–4768
33. Shimokawa, T., Kulmacz, R. J., DeWitt, D. L., and Smith, W. L. (1990) *J. Biol. Chem.* **265,** 20073–20076
34. Weller, P. E., Markey, C. M., and Marnett, L. J. (1985) *Arch. Biochem. Biophys.* **243,** 633–643
35. Marnett, L. J., Siedlik, P. H., Ochs, R. C., Pagels, W. D., Das, M., Honn, K. V., Warnock, R. H., Tainer, B. E., and Eling, T. E. (1984) *Mol. Pharmacol.* **26,** 328–335
36. Hsuanyu, Y., and Dunford, H. B. (1990) *Biochem. Cell Biol.* **68,** 965–972
37. Antholine, W., Mailer, C., Reichling, B., and Swartz, H. N. (1976) *Phys. Med. Biol.* **21,** 840–846
38. Odenwaller, R., Chen, Y.-N. P., and Marnett, L. J. (1990) *Methods Enzymol.* **187,** 479–485
39. DeGray, J. A. (1987) *Computer Stimulations as an Aid to ESR Powder Pattern Analysis of Some Organocobalt and Organopalladium Complexes.* Ph.D. thesis, Brown University, Providence, RI
40. Rieger, P. H. (1982) *J. Magn. Res.* **50,** 485–489
41. Eling, T. E., Curtis, J. F., Harman, L. S., and Mason, R. P. (1986) *J. Biol. Chem.* **261,** 5023–5028
42. Lassmann, G., Liermann, B., and Langen, P. (1989) *Free Rad. Biol. Med.* **6,** 9–14
43. Graslund, A., Sahlin, M., and Sjöberg, B.-M. (1985) *Environ. Health Perspect.* **64,** 139–149
44. Ehrenberg, A. (1986) in *Thioredoxin and Glutaredoxin Systems: Structure and Function* (Holmgren, A., ed) p. 209, Raven Press, New York
45. Bender, C. J., Sahlin, M., Babcock, G. T., Barry, B. A., Chandrashekar, T. K., Salowe, S. P., Stubbe, J., Lindstrom, B., Petersson, L., Ehrenberg, A., and Sjöberg, B.-M. (1989) *J. Am. Chem. Soc.* **111,** 8076–8083
46. Fasanella, E. L., and Gordy, W. (1969) *Proc. Natl. Acad. Sci. U. S. A.* **62,** 299–304
47. Barry, B. A., El-Deeb, M. K., Sandusky, P. O., and Babcock, G. T. (1990) *J. Biol. Chem.* **265,** 20139–20143
48. Barry, B. A., and Babcock. G. T. (1988) *Chem. Scr.* **28A,** 117–122
49. Miki, H., Harada, K., Yamazaki, I., Tamura, M., and Watanabe, H. (1989) *Arch. Biochem. Biophys.* **275,** 354–362
50. Markey, C. M., Alward, A., Weller, P. E., and Marnett, L. J. (1987) *J. Biol. Chem.* **262,** 6266–6279
51. Egan, R. W., Paxton, J., and Kuehl, F. A., Jr. (1976) *J. Biol. Chem.* **251,** 7329–7335
52. Chen, Y.-N. P., and Marnett, L. J. (1989) *FASEB J.* **3,** 2294–2297
53. Hemler, M. E., Graff, G., and Lands, W. E. M. (1978) *Biochem. Biophys. Res. Commun.* **85,** 1325–1331
54. Fishel, L. A., Farnum, M. F., Mauro, J. M., Miller, M. A., Kraut, J., Liu, Y., Tan, X., and Scholes, C. P. (1991) *Biochemistry* **30,** 1986–1996
55. Ingold, K. (1969) *Acc. Chem. Res.* **2,** 1–9
56. Hamberg, M., and Samuelsson, B. (1967) *J. Biol. Chem.* **242,** 5344–5354
57. Lands, W. E. M., Lee, R., and Smith, W. L. (1971) *Ann. N. Y. Acad. Sci.* **180,** 107–122
58. Lands, W. E. M., Kulmacz, R. J., and Marshall, P. J. (1984) in *Free Radicals in Biology* (Pryor, W. A., ed) Vol. 6, pp. 39–61, Academic Press, New York
59. Chen, Y.-N. P., Bienkowski, M. J., and Marnett, L. J. (1987) *J. Biol. Chem.* **252,** 16892–16899